We are IntechOpen, the world's leading publisher of Open Access books
Built by scientists, for scientists

4,800
Open access books available

122,000
International authors and editors

135M
Downloads

Our authors are among the

154
Countries delivered to

TOP 1%
most cited scientists

12.2%
Contributors from top 500 universities

CLARIVATE ANALYTICS
BOOK CITATION INDEX
INDEXED

WEB OF SCIENCE™

Selection of our books indexed in the Book Citation Index
in Web of Science™ Core Collection (BKCI)

Interested in publishing with us?
Contact book.department@intechopen.com

Numbers displayed above are based on latest data collected.
For more information visit www.intechopen.com

Biophysical Properties of the Basal Lamina: A Highly Selective Extracellular Matrix

Fabienna Arends and Oliver Lieleg

Additional information is available at the end of the chapter

Abstract

In this chapter, we discuss a specialized version of the extracellular matrix, the basal lamina. We focus on biophysical approaches which helped in identifying the mechanistic principles that allow the basal lamina to act as a selective permeability barrier. We discuss the physicochemical interactions that entail binding of molecules or nanoparticles to the basal lamina matrix and outline physiological scenarios where altered selective permeability properties of the basal lamina might contribute to physiological (mal) function.

Keywords: laminin, collagen, entactin, microstructure, viscoelastic properties, permeability

1. Molecular composition of the basal lamina

The basal lamina constitutes a thin extracellular matrix, which is located between the connective tissue and the basolateral side of a cell layer. This cellular layer can consist of either endothelial or epithelial cells, and those cell types secrete the different molecular components of the basal lamina. The main components of the basal lamina are laminin, collagen IV, the perlecan complex, and entactin, which are also known as nidogen [1, 2]. Together, those macromolecules form a complex network as illustrated in **Figure 1**. In addition, the basal lamina may contain several proteases such as matrix metalloproteinase-2 (MMP-2), MMP-9, and growth factors such as transforming growth factor beta (TGF-β), insulin-like growth factor (IGF) and fibroblast growth factor (FGF) [3].
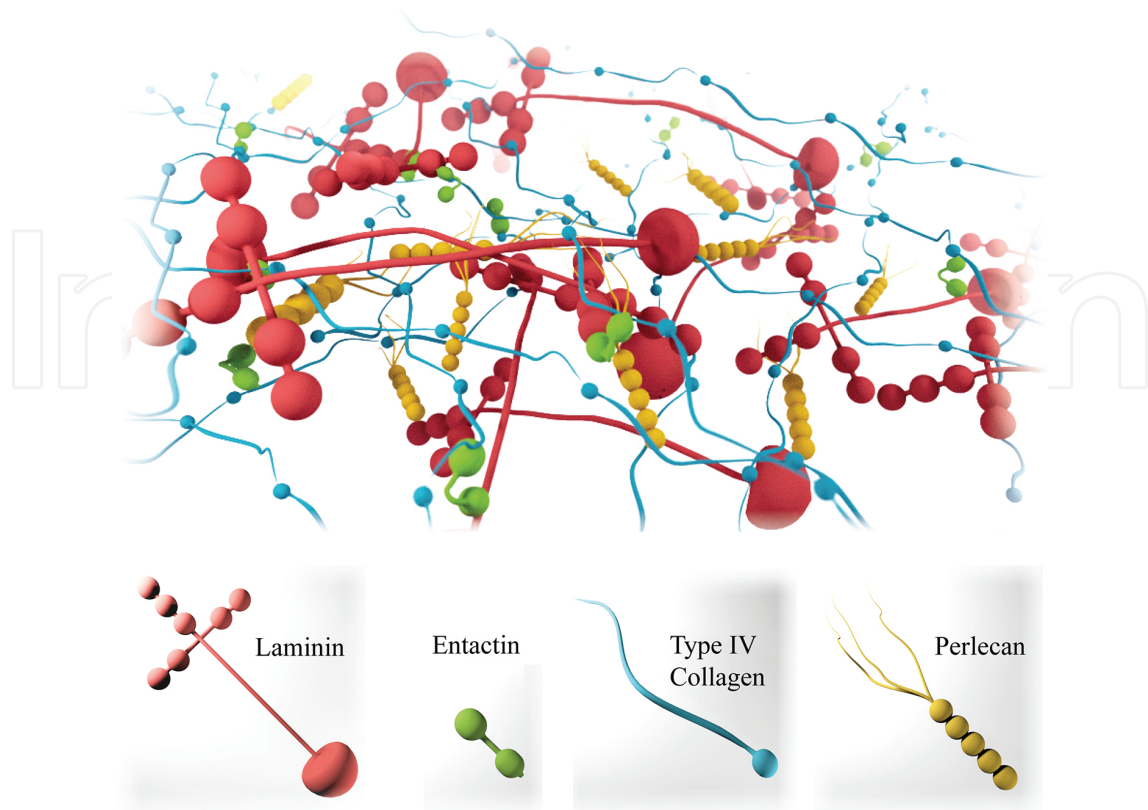
Figure 1. Schematic illustration of the basal lamina network. Both laminin and collagen IV assemble into a sheet-like network. Those two networks are cross-linked by entactin as well as the perlecan complex.

Laminin is a glycoprotein mainly found in basement membranes such as the basal lamina and is composed of three polypeptide chains: α-chain, β-chain, and γ-chain [4]. These three chains assemble into a cross-like structure, where the short arms of the cross are formed by the N-termini of the three subunits. The long arm of this cross-like structure is formed by all three subunits which assemble into an α-helical coiled-coil structure with a globular end [4, 5]. Laminin self-assembles into a sheet-like structure by binding the short arms of different laminins to each other [6]. The polymerized laminin network is anchored to the underlying cell layer via integrin interactions mediated by the globular end of the cross-like structure [4, 7]. Collagen IV is a collagen variant mostly found in the basal lamina and forms a helix similar to collagen I [8]. Type IV collagen self-assembles via covalent bonding, disulfide cross-linking, and non-covalent side-by-side interactions into a sheet-like structure [2]. Both sheet-like structures, the laminin and collagen IV network, do not interact with each other; however, both laminin and collagen IV can bind to perlecan as well as entactin. As a consequence, the latter two molecules act as cross-linkers between the two sheet-like structures, thus maintaining the complex architecture of the basal lamina [9]. The perlecan complex is a basal lamina-specific proteoglycan. In general, proteoglycans consist of a protein core with glycosaminoglycans covalently attached to the protein. Thus, the perlecan complex consists of perlecan as core protein and 2–15 heparan sulfate (HS) side chains [10]. Also entactin is a glycoprotein and consists of three globular units connected by rod-like structures [11]. Two of

the three globular units (G1 and G2) are situated at the N-terminus of entactin. The third globular unit (G3) is found at the C-terminus of the protein. G3 strongly binds to the γ-laminin short arm but can also bind to collagen IV. In contrast, G2 only binds to collagen type IV [11], thus connecting the networks built by laminin and collagen type IV.

In addition to building a complex network and serving as an anchoring matrix for a neighboring cell layer, all of these basal lamina components can directly influence the cell fate: laminin, in combination with collagen IV supports cell attachment, differentiation, migration, and growth [12]. It was suggested that in addition to fibronectin, type IV collagen and laminin are involved in the formation of tight junctions [13]. Laminin and collagen IV are also key players in establishing the mechanical stability of the basal lamina [10]. As mentioned above, the proteoglycan perlecan consists of a core protein to which HS, a heavily charged glycosaminoglycan, is attached. In addition to acting as a cross-linker between laminin and collagen IV, perlecan and, in particular, the highly charged HS chains are responsible for the hydration of the matrix and contribute to the selective filtering properties of the basal lamina [14–16].

Although this highly specific structure–function relationship suggests that the microarchitecture of the basal lamina might be rather static, proteolysis of extracellular matrix (ECM) components and thus matrix remodeling is a process which continuously takes place *in vivo*. Remodeling of the ECM is, for example, a crucial part of wound healing and cell differentiation [17]. In addition, the degradation of ECM components can be responsible for cell apoptosis but, depending on the ECM component degraded, can also enhance cell viability [18]. In particular, the degradation of laminin is thought to be harmful for cells: In a study conducted in mice, it was suggested that the breakdown of laminin by the MMP-9 induces neuronal apoptosis but can be prevented by the addition of MMP-9 inhibitors [19].

Moreover, the degradation of laminin does not only result in cell apoptosis but also impacts the stability of the basal lamina [20]. Since laminin interacts with the integrins on the cell surface and anchors the cells onto the basal lamina, a breakdown of laminin results in a separation of the basal lamina from the endothelial/epithelial cell layer which in turn induces a loss of cell–matrix communication [21, 22]. It was shown in an *in vivo* study in a mouse model that when the second structural main component of the basal lamina, collagen IV, is knocked out, embryos develop normal during the first few days, but after 10 days of development lethality occurs [23]. It was suggested that collagen IV is essential for the function and integrity of the basal lamina when mechanical stress increases. However, collagen IV seems to be unimportant in the assembly of the basal lamina at early embryonic states [23]. Similar results were obtained when an enzyme, which catalyzes the assembly of collagen IV, was modified and thus nonfunctional. In these mice, collagen IV was present but did not assemble properly and the mouse embryos died after 10 days [24].

In contrast to those structural main components, loss of the small cross-linking molecule entactin seems to have a weaker influence on basal lamina structure and function. In mice, the inactivation or mutation of the gene encoding entactin results in a normal basal lamina phenotype, and the viability of the mutant mice seems not be strongly impaired by a loss of entactin [25–27]. Exceptions are the lung and the kidney, organs which fulfill important filtering tasks and thus contain a huge amount of basal lamina. Here, a loss of entactin cross-

linking function entailed strong alteration of those tissues during embryonal development and ultimately led to death immediately after birth [28]. Of course, alterations in basal lamina properties can also have less severe consequences. For instance, long-term diabetes patients not only often suffer from retinopathies but also show an increased thickness and stiffness in the ocular basal lamina. Here, however, the higher amount of basal lamina proteins is due to the expression of diabetes-specific proteins whereas the production of the normal basal lamina components is not increased [29].

2. Selective permeability of the basal lamina *in vivo*

In the human body, the basal lamina always supports a cell layer of either endothelial or epithelial cells (**Figure 2**). Together, these two layers form a complex barrier which selectively regulates the entrance and distribution of molecules from or into the connective tissue. Molecules which are selectively transported across the basal lamina include growth factors, nutrients, and hormones. Examples for such basal lamina/cell barriers are found in the skin, the kidney, the blood–brain barrier, and the vascular system [10, 30–34].
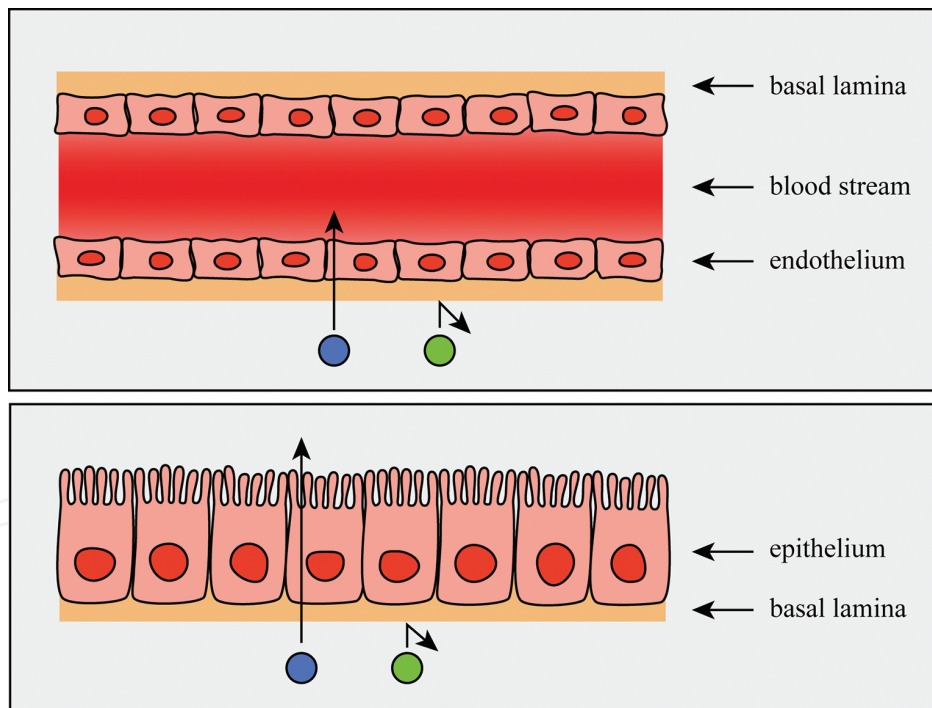
Figure 2. Illustration of complex barriers consisting of a cell layer and an adjacent basal lamina layer. The inner layer of blood vessels is constituted by endothelial cells with a basal lamina layer located on the outer side of the blood vessel. Also epithelial cells are supported with a thin layer of basal lamina. In both examples, selective permeability of the complex cell/biopolymer barrier toward molecules is observed, that is, some molecules can penetrate the barrier whereas others are rejected.

The skin poses one of the largest and, in most cases, the first barrier for foreign compounds. In addition to this protective function, the skin also regulates the uptake of oxygen and

prevents the loss of water from the underlying tissue [32]. In kidney tissue, the basal lamina is, in combination with the epithelial cells, responsible for filtering [10], and defects in the basal lamina can result in kidney malfunction [34]. The blood–brain barrier [30] protects the brain tissue from pathogens and neurotoxic molecules, whereas it allows the passage of regulatory molecules such as hormones from the blood stream into the cerebrospinal fluid [35]. A similar structure is present in the vascular system. Here, the first barrier is established by endothelial cells which rest on a thin layer of basal lamina on their basolateral side [10]. Nutrients, growth factors, proteins, hormones, and polysaccharides are prevented from leaking from the blood stream into the connective tissue by tight junctions between the endothelial cells [31, 35–37]. If the integrity of these tight junctions is impaired, the basal lamina becomes directly accessible for blood compounds. Moreover, if the basal lamina layer is damaged, the translocation of solutes from the blood stream into the connective tissue is increased, even if the tight junctions are intact [20]. Of course, for molecules which need to traverse from the connective tissue into the blood stream, the basal lamina is encountered first before the endothelial cells are reached. In this scenario, the basal lamina layer constitutes the primary barrier.

A detailed knowledge of the molecular interactions which determine the selective filtering properties of the basal lamina is especially interesting for the design of new drug carrier vehicles for targeted drug delivery applications. One example for such an application is the specific targeting of tumors. In tumor tissue, the influence of the basal lamina barrier becomes even more important since tumors usually show an increased production of ECM [38]. Drug carriers are often injected intravenously; thus, the vascular system poses the critical barrier which the drug carriers have to pass. Here, the passage of drugs/drug carrier vehicles from the blood stream into the adjoining tissue is primarily regulated by the endothelial cells. However, in most cases, the endothelium around tumors is leaky. This is also known as an "enhanced permeability and retention effect" (EPR). Since the barrier function of the endo-thelium is impaired by the tumor, the basal lamina becomes directly accessible for compounds from the blood stream. In such a situation, the passage of drug carrier systems and their incorporated drugs is mainly regulated by the basal lamina.

In all of these examples, the selective barrier properties of the basal lamina are key for regulating complex biological processes. To possess such a high selectivity toward molecules or drug carrier particles, that is, deciding which of them are allowed to pass and which are rejected, an advanced molecular filter system based on various interactions is needed. Understanding the physical interactions between drug carriers and the complex multicom-ponent, basal lamina is crucial to efficiently adjust the surface parameters of drug carriers in such a way either that they are able to easily penetrate the basal lamina barrier or that they accumulate at the basal lamina interface. Studying the mechanistic principles which govern the selective permeability properties of the basal lamina layer *in vivo* is, however, very difficult: On the one hand, the basal lamina has a thickness of only a few hundred nanometers which would require optical experiments with a supreme spatial resolution such as PALM/STORM or STED microscopy [39]. On the other hand, the presence of a plethora of molecules, dynamic alterations in the basal lamina composition by enzymatic processes, or generation of new basal lamina components by the adjacent cell layer further complicates the interpretation of *in vivo*

permeability studies and the correlation of the experimental results with physicochemical principles. Thus, a detailed investigation of the selective permeability properties of a complex biopolymer barrier such as the basal lamina requires a reliable *in vitro* model system, which is available in quantities large enough to conduct systematic tests while reproducing the behavior of the *in vivo* basal lamina layer.

3. Basal lamina model systems

A suitable source for the purification of an extracellular matrix that mimics the basal lamina is the Engelbreth–Holm–Swarm sarcoma of mice. This tumor produces, in contrast to healthy tissue, large amounts of ECM with laminin and collagen IV being the main components [3]. Depending on the question asked, individual macromolecular components of the basal lamina may be sufficient to take over the role of the complex biopolymer mixture. For instance, adhesion of cells to solid substrates is promoted similarly well by laminin coatings as by coatings with the multicomponent ECM [40, 41]. For other basal lamina properties such as viscoelasticity and selective permeability, it is crucial that the biological complexity of the system is maintained so that the full spectrum of basal lamina function is obtained.

The high abundance of ECM in Engelbreth–Holm–Swarm tumor tissue makes it possible to purify reasonable amounts of this multicomponent matrix as required for systematic *in vitro* experiments. A first purification protocol for this ECM was established by Kleinman et al. [42, 43] in the 1980s. The extract is liquid at temperatures between 4°C and approx. 15°C and forms a gel at higher temperatures. In its gel form, the matrix was tested for its biological activity, and it was shown in several studies that the purified ECM successfully promotes the differentiation of various cell types [44–47]. Cells can be either plated on top of the gel, thus simulating a two-dimensional (2D) environment, or they can be embedded into a 3D ECM matrix. Which configuration is chosen depends on the detailed experimental setup, the cell type used and the biological question. For instance, cell migration experiments can be conducted both on flat surfaces which have been coated by ECM components and in 3-dimensional basal lamina gels [48, 49].

The purification protocol of Kleinman et al. is used by several companies for the commercial production of ECM. Although these commercial ECM variants are extracted according to the same purification protocol, significant differences in the behavior of cells embedded into those gels have recently been described [50]: The migration behavior of leukocyte-like dHL-60 cells in four different commercially available ECM gel variants differed strongly even though the gels were prepared at matching total protein concentrations. Moreover, in one of the ECM gels, life–dead stains demonstrated a significantly increased percentage of nonviable cells. At the same time, for this gel variant, there was an additional band visible when the gel was analyzed by SDS-PAGE. Mass spectrometry showed that this additional band contained laminin fragments which indeed are suspected to be harmful for cells. This result demonstrates the dilemma a researcher is exposed to when working with commercial model systems: On the one hand, the relatively easy availability of the material in reasonable quantities allows for conducting *in vitro* experiments which otherwise would not be possible. On the other hand,

comparability to results from other researchers is often difficult if different vendor sources for the biopolymer mixture are used: The data obtained need to be interpreted with great care and ideally should be double-checked with a second, independent ECM preparation. SDS-PAGE analysis also suggested that the commercial ECM variants differed in terms of the relative concentration of basal lamina components. Whereas, in all ECM preparations, the bands corresponding to collagen IV and laminin were clearly most pronounced, the strongest variability occurred in a band around 50 kDa which matches the molecular weight of entactin. Since this molecule acts as a cross-linker between laminin and collagen IV, it is reasonable to assume that variations in its relative concentration will also affect the structure and permeability properties of the ECM gels and, ultimately, the migration behavior of cells in those gels. However, biochemical techniques are not able to predict those gel parameters, which is why physical methods are required to further characterize the different basal lamina model systems.

4. Physical properties of basal lamina gels *in vitro*

In addition to the biochemical structure of its constituents, the following three physical parameters dictate the behavior of molecules, nanoparticles, or cells within the basal lamina: the microstructure, the mechanical properties, and the permeability of the hydrogel. In biopolymer networks, the microstructure of the system has direct implications on both the viscoelastic properties of the network [51] and its permeability properties [31]. Thus, imaging methods for visualizing biopolymer networks such as the basal lamina are discussed first.
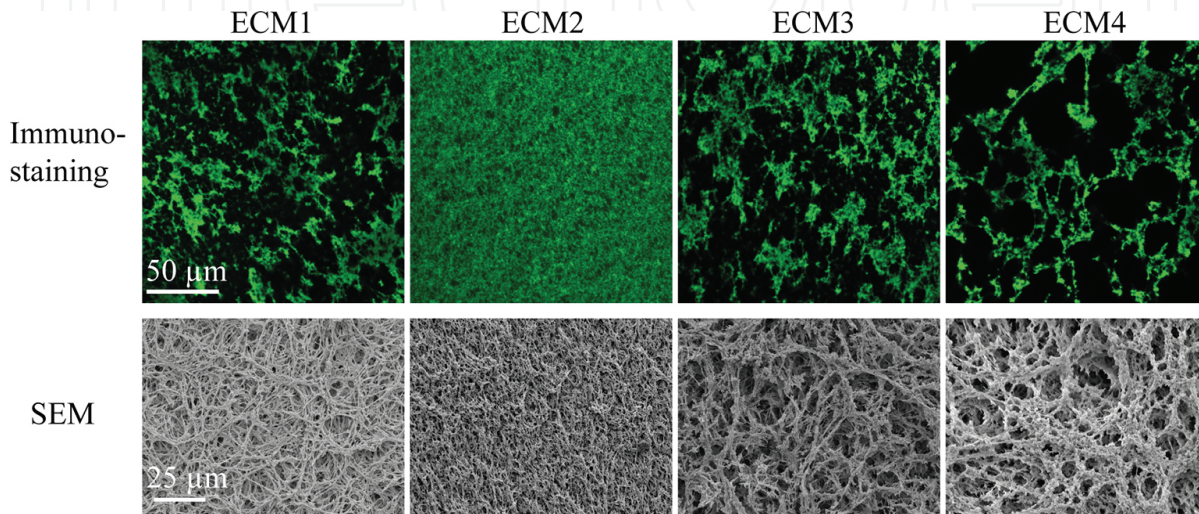
4.1. Microstructure of ECM gels

There are various methods to evaluate the structure of a material, and those methods can be subdivided into the following categories: surface imaging techniques, near-field/contact-based techniques and far-field imaging. Which method is used to resolve the structure depends on the material and on the experimental question: Do I require information on the surface topology or on the inner structure of the material? For biological samples, a fixation is needed for most of the imaging techniques so that the structure does not change over time or during the sample preparation process. One technique which is often used to image biological samples is fluorescence confocal microscopy as this method can visualize the 3D structure of a biopolymer network. However, most biological samples are not fluorescent by themselves and thus a fluorescent dye has to be used to stain the structure of interest. For many target proteins, commercial antibodies are available to which a fluorescent dye is attached. Before such a staining with antibodies is performed, the samples are typically fixed to ensure that the structure of the biopolymer network is not altered by the antibody application and the following washing step.

A suitable technique for imaging the surface of a biopolymer material is scanning electron microscopy (SEM). For this technique, the sample surface needs to be electrically conductive. Since this is typically not the case for biological samples, the application of a thin conductive

layer, for example gold, is necessary. Depending on the type of SEM used for imaging, the samples are also exposed to a vacuum for imaging; this requires sample fixation and subsequent dehydration as typical additional preparation steps for this imaging method. It is clear that sample preparation steps necessary for both imaging techniques may introduce artifacts, that is, alterations of the microstructure of the biopolymer network. However, as the preparation steps for both techniques are different, the obtained pictures are reliable if both imaging methods return comparable structures.

Figure 3. Microstructure of four ECM gel variants. Images obtained with immunostaining/confocal microscopy and with a SEM are compared. Both methods show a denser network for the gel variant 2 (ECM2) than for the other three variants. Edited figure with permission from Arends et al. [50]. © 2015 Arends et al. Published under CC BY license.

Example images of basal lamina model systems are shown in **Figure 3**, where the microstructure of four different ECM gel variants is compared. For the fluorescent confocal image, the ECM component laminin was stained with a fluorescent antibody and an optical slice with a thickness of 0.9 μm was acquired inside the 3-dimensional gel. Here, the ECM variant in which leukocyte migration was slowed down most (ECM2) shows the lowest porosity. The same difference in the microarchitecture of the ECM gels is obtained when SEM is used for imaging: ECM2 shows the highest density, whereas the other gel variants exhibit a comparable network structure. As the four gel variants have all been reconstituted at identical total protein concentrations, the observed structural difference is most likely due to the higher content of the cross-linking molecule entactin in this ECM variant as detected by SDS-PAGE.

4.2. Viscoelastic properties of ECM gels

Especially for cell differentiation, the mechanical properties of the ECM play an important role. Using artificial hydrogels such as cross-linked polyacrylamide gels [52], it was shown that cell differentiation can be directed by the stiffness of the substrate. The ECM is a viscoelastic material, that is, its mechanical behavior combines both viscous as well as elastic properties. Those viscoelastic properties can be probed macroscopically with a shear rheometer as

illustrated in **Figure 4** as well as microscopically with single-particle tracking microrheology or AFM indentation.

In macroscopic shear rheology, the sample is placed between two plates, a stationary bottom plate and a rotating top plate for shear stress application. The bottom plate can be heated or cooled depending on the desired temperature conditions. The top plates are available in various diameters and shapes and are chosen according to the sample properties and the quantity to be measured. For determining viscoelastic properties, the top plate is typically oscillated at different frequencies, either at a fixed strain or at a fixed torque. Small torques during such a measurement ensure that the material response is quantified in the linear response regime, where Hooke's law holds, that is, where the ratio of stress and strain is independent from the amplitude of the applied force.
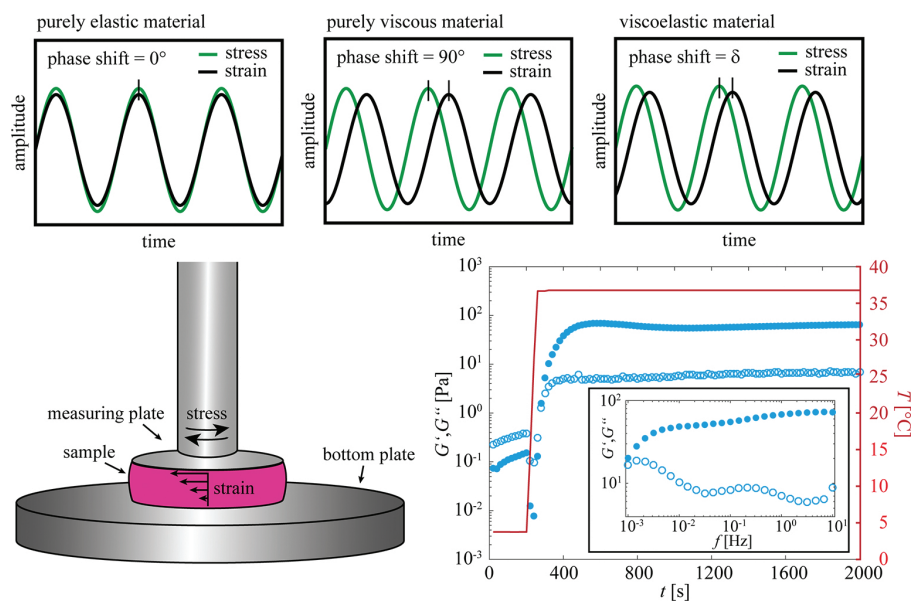
Figure 4. The viscoelastic behavior of ECM gels can be quantified by shear rheology. The sample is placed between a stationary bottom plate and a measuring plate, and then, an oscillating shear stress is induced. The temporal delay (phase shift) of the material response is measured. For a purely elastic material, the phase shift is 0°; in contrast, a phase shift of 90° is obtained for a purely viscous substance. For a viscoelastic material, the phase shift can assume any value between 0° and 90° (adapted from an illustration by Stefan Grumbein). A typical gelation curve for a basal lamina gel at a concentration of 8.3 mg/mL is shown at the bottom right and was acquired using a plate–plate geometry oscillating at a frequency of 1 Hz. For the first 200 s, the measurement was performed at 4°C. At this temperature, the ECM is in its liquid state, thus the loss modulus (open circles) dominates over the storage modulus (full circles). When the temperature is increased to 37°C, gelation is initiated and the storage modulus dominates. After a few minutes, a plateau value is reached. A typical frequency spectrum after gelation is shown as inset. The storage modulus dominates over the loss modulus over four decades of frequencies.

The viscoelastic properties of the ECM can then be described by the storage modulus G' and the loss modulus G''. Here, G' is a measure for the elastic properties and G'' for the viscous properties of the ECM gel. At low temperatures around 4°C, the ECM is in a liquid state. Here, its viscous properties dominate and the loss modulus is larger than the storage modulus. When the ECM gel is heated to room temperature or above, a gelation process is initiated which results in an increased storage modulus: Within a few minutes after the temperature increase

is applied, the storage modulus starts to dominate over the loss modulus and then increases further until it reaches a plateau value (see **Figure 4**). In general, there are several parameters determining the absolute value of the plateau elasticity: The higher the concentration of proteins/polymers the higher is typically the storage modulus [53]. In addition to the concentration of protein, also the type of polymer/polymer interaction plays a role. The storage modulus of an entangled solution is usually lower than for a cross-linked network. In the study conducted in [50], it was shown that the amount of the cross-linking molecule entactin influences the network stiffness: The higher the concentration of entactin the higher the storage modulus and thus the elasticity of the formed matrix. Typical values for the elastic modulus obtained for ECM gels at a total protein concentration of 3.5 mg/mL are in the range of 1-10 Pa which is very soft and lies in the range of moduli reported to induce neuron-like differentiation of stem cells [52].

In general, the viscoelastic properties of a biopolymer network may depend strongly on the probing frequency [51], especially if the network constituents are only entangled. For cross-linked systems, however, a pronounced plateau in the frequency-dependent shear moduli is expected, and exactly such behavior is also observed for ECM gels (**Figure 4**).

The absolute values of the viscoelastic parameters obtained with macrorheology may not necessarily reflect the local stiffness of a biopolymer network. Thus, microrheological techniques such as bead microrheology [54] or AFM nanoindentation [55] have been introduced and already applied to other biopolymer systems such as cytoskeletal networks [56–58] or cartilage [59]. With those nano-/microscopic techniques, it is also possible to spatially map the mechanical properties of native basement membranes [60, 61], which might give insights important for cellular processes such as differentiation or migration.

4.3. Permeability of ECM gels

One of the major tasks of the basal lamina is to act as a molecular filter. Here, the exclusion of particles or molecules according to their size is one of the simplest mechanisms for establishing permeability: A mesh size smaller or in the order of the particle diameter will prevent the entrance of particles into the network; conversely, if particles have already entered the network, they will be efficiently trapped within the biopolymer matrix. However, this filter mechanism is not very sophisticated as it cannot differentiate between objects of the same size. Thus, a second filter mechanism based on binding interactions between diffusing particles/molecules and the basal lamina constituents has been put forward to contribute to the selective permeability properties of biopolymer hydrogels such as the basal lamina [31]. With the ECM model system discussed above, the physicochemical principles governing the high selectivity of basal lamina gels can be studied systematically.

To probe the interactions between particles and the ECM, single-particle tracking (SPT) can be employed. In contrast to SPT used for microrheology [62], the diameter of the particles embedded into the ECM should be small compared to the mesh size of the gel. Only then one can be sure that the particle motion is not geometrically restricted by the network microarchitecture—which demonstrates the importance of obtaining structural information on the system prior to commencing SPT experiments. In SPT measurements, the diffusive movement

of particles within the gel is recorded via light microscopy and every single particle is evaluated separately. The trajectory of motion of each particle, in particular the x- and y-position, is extracted from recorded movies for every frame of the movie—typically over a time course of several seconds up to a minute (depending on the temporal resolution of the image acquisition process, **Figure 5**). These data are then used to calculate the mean squared displacement (*MSD*) of every particle according to the following

$$MSD(\tau) = \frac{1}{N} \sum_{i=1}^{N} [\bar{r}(i\Delta t + \tau) - \bar{r}(i\Delta t)]^2$$

(1)

Here, N denotes the total number of recorded frames, $\overset{\circ}{r}(t)$ is the position of the particle at time t, and τ denotes the time interval between two particle positions within a given trajectory. For diffusive processes, the *MSD* typically grows with time as a power law τ^α, with the exponent α characterizing the type of diffusive motion: One can distinguish sub-diffusive ($\alpha<1$), normal diffusive ($\alpha=1$), or superdiffusive behavior ($\alpha>1$), the latter of which is typically linked to active transport phenomena or liquid flow.

Such SPT experiments revealed that both positively and negatively charged microparticles were efficiently immobilized in the ECM gel, whereas PEGylated (and thus only weakly charged) polystyrene particles of identical size were able to diffuse almost freely within the gel [63]. Equivalent results were obtained with liposome particles and suggested that free diffusion within the ECM matrix is only possible as long as the particle surface charge (as quantified by the zeta potential) lies within a window ranging from intermediate negative charge to low positive charge. Enzymatic digestion of the ECM component HS entailed a mobilization of positively charged particles. This finding suggested that the polyanionic HS chains present in the perlecan complex critically contribute to the selective properties of the ECM gel—likely through trapping of positively charged objects by means of electrostatic binding.

The notion that electrostatic binding interactions contribute to particle trapping in ECM gels was confirmed by experiments conducted at elevated ionic strength of the hydrogel buffer. Increased salt concentrations lead to charge screening effects by the formation of a layer of counter ions around the surface of charged objects such as particles or hydrogel polymers. As a consequence, the strength of electrostatic interactions at a given separation distance between two objects is reduced—a process which is described by the Debye–Hückel theory [64]. At physiological concentrations of KCl, both positively and negatively charged polystyrene microparticles are immobilized in ECM gels. However, when the KCl concentration is increased, a fraction of the particles becomes mobile [63, 65]. This mobilization does not have to be permanent as individual particles can dynamically switch between a freely diffusing and bound state over time, and—while in the bound state—also between a weakly and strongly bound configuration. As shown in **Figure 5**, the degree of particle mobilization depends both on the ion concentration and valency which is consistent with the Debye–Hückel theory. However, particle mobilization efficiency seems also to depend on the particular ion species

as identical concentrations of the divalent ions Mg^{2+} and Ca^{2+} lead to different experimental outcome [65]. This ion-specific effect suggests that, in addition to electrostatic forces, also hydrophobic interactions are likely to contribute to the selective filtering properties of the basal lamina.

Systematic permeability studies with artificial particles were very helpful to unravel the physical mechanisms which are responsible for the trapping of solutes in the basal lamina. However, most compounds which encounter the basal lamina layer under physiological conditions are small molecules rather than microparticles. To investigate the selective properties of the basal lamina toward small molecules, a microfluidic setup (**Figure 6**) was recently introduced [66]. Here, customized peptides with tailored amino acid sequences and thus different net charges were used as diffusion probes. To ensure optimal comparability, the molecular weight of those oligopeptides was kept constant. The penetration behavior of those peptides into an ECM gel was visualized by fluorescent microscopy, and similar to the SPT experiments discussed above also the behavior of those molecules critically depended on their charge. Positively charged peptides accumulated at the gel/buffer interface, whereas nega-
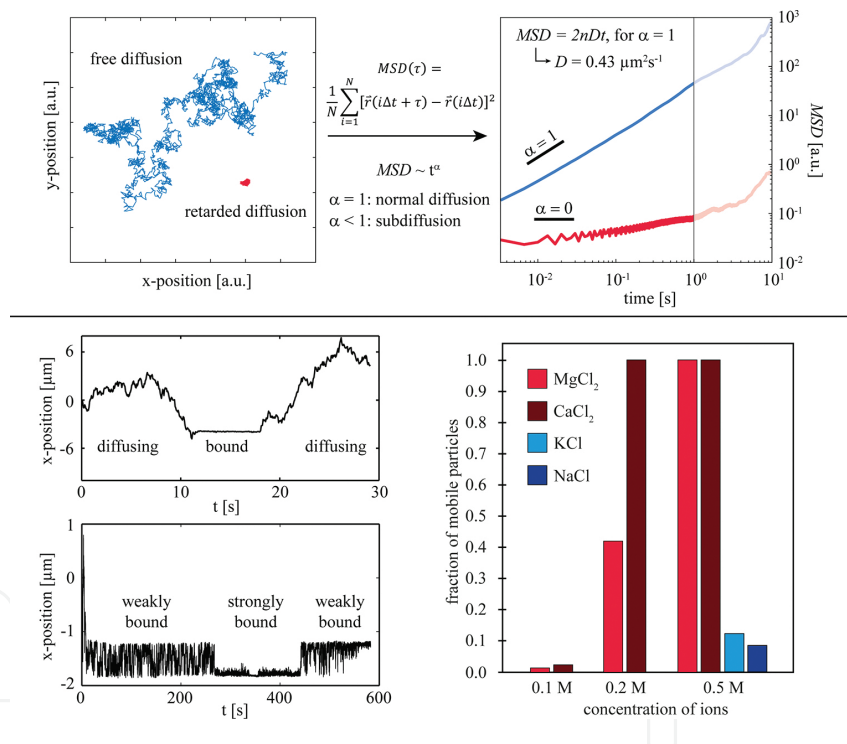

Figure 5. Single-particle tracking experiments can locally map the permeability of ECM gels. *Upper panel*: Exemplary trajectories and the corresponding MSD curves of a particle showing free diffusion and a particle showing retarded diffusion. For freely diffusing particles, the dependence of the MSD on time is linear and a diffusion coefficient D can be calculated according to the formula shown in the graph. For the calculation of D, only the first 10% of the MSD data is used to avoid errors arising from statistical uncertainties. *Lower panel*: Trajectories of a particle which transiently switches between a diffusing and a bound state and of a particle which alternates between a strongly and a weakly bound configuration. The states of motion can be distinguished based on the fluctuation amplitude of the particle. Both trajectories were obtained at a salt concentration of 1 M KCl. The histogram shows that in ECM gels, the fraction of mobile particles depends on the concentration, valency, and detailed species of the ions used. Adapted with permission from Arends et al. [65]. Copyright ©2013 American Chemical Society.

tively charged peptides did not. Moreover, when the net charge of the positively charged peptides was increased, the accumulation propensity of the molecules at the gel interface was increased as well. Of course, such an artificial microfluidic setup does not reproduce the complex situation of the basal lamina interface found *in vivo*. However, peptide injection tests in the connective tissue of living mice demonstrated a similar charge-selective accumulation behavior at the basal lamina layer of blood vessels as observed on-chip with the simplified ECM/buffer interface. This underscores the great potential basal lamina model systems and biophysical characterization methods hold for gaining a better insight into the mechanistic principles that establish the complex properties of the basal lamina.

5. Outlook

Here, we have summarized selected aspects of our current understanding how the biochemical composition of the basal lamina is mirrored in the complex microarchitecture as well as the multi-facetted material properties of the biopolymer network. Deciphering the physicochemical principles which dictate the microstructure, viscoelastic properties, and selective perme-ability of the basal lamina layer are not only interesting for cell biology studies [67, 68], drug
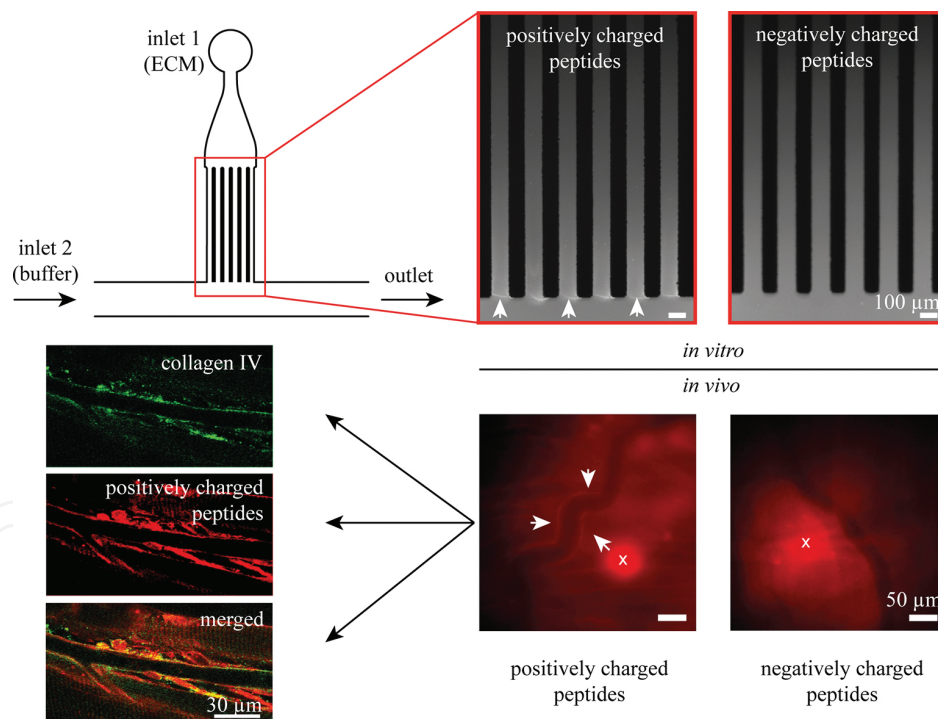
Figure 6. Illustration of a microfluidic setup used to probe the diffusive penetration of peptides from a buffer compart-ment into a basal lamina gel. Typical intensity profile images for positively and negatively charged peptides are shown next to the microfluidic channel. For positively charged peptides, an intensity peak is observed at the buffer/gel inter-face, whereas such an accumulation does not occur for negatively charged peptides. Similar results are obtained when those peptides are injected into the connective tissue of mice. Tissue immunostaining confirmed that the positively charged peptides colocalize with collagen IV, a main component of the basal lamina. Adapted with permission from Arends et al. [66]. © 2015 Arends et al. Published under CC BY license.

delivery questions and tumor treatment [69–72], but might also have strong implications for tattoo removal applications: Here, ink nanoparticles trapped in the skin tissue have to be mobilized, for example, by soaking the tissue in salt solutions, so that they can be washed out from the skin rather than removed by painful and scar-inducing laser treatment. The lessons learned from systematically unraveling the physical and chemical mechanisms, which give rise to the complex properties of the basal lamina, may also help in the rational design of artificial hydrogel systems for tissue engineering approaches: The synthesis of complex macromolecules with well-defined chemical properties may allow for constructing hydrogels with both tailored mechanical properties and selective permeability behavior.

Acknowledgements

Author details

Fabienna Arends[1,2] and Oliver Lieleg[1,2*]

*Address all correspondence to: oliver.lieleg@tum.de

1 Institute of Medical Engineering IMETUM, Technical University of Munich, Boltzmannstrasse 11, Garching, Germany

2 Department of Mechanical Engineering, Technical University of Munich, Boltzmann-strasse 15, Garching, Germany

References

[1] Timpl R. Macromolecular organization of basement membranes. Current Opinion in Cell Biology. 1996;8(5):618–24.

[2] Yurchenco PD, Orear JJ. Basal lamina assembly. Current Opinion in Cell Biology. 1994;6(5):674–81.

[3] Kleinman HK, Martin GR. Matrigel. Basement membrane matrix with biological activity. Seminars in Cancer Biology. 2005;15(5):378–86.

[4] Aumailley M. The laminin family. Cell Adhesion & Migration. 2013;7(1):48–55.

[5] Paulsson M, Deutzmann R, Timpl R, Dalzoppo D, Odermatt E, Engel J. Evidence for coiled-coil alpha-helical regions in the long arm of laminin. The Embo Journal. 1985;4(2):309–16.

[6] Cheng YS, Champliaud MF, Burgeson RE, Marinkovich MP, Yurchenco PD. Self-assembly of laminin isoforms. Journal of Biological Chemistry. 1997;272(50):31525–32.

[7] Aumailley M, Pesch M, Tunggal L, Gaill F, Fassler R. Altered synthesis of laminin 1 and absence of basement membrane component deposition in beta 1 integrin-deficient embryoid bodies. Journal of Cell Science. 2000;113(2):259–68.

[8] Khoshnoodi J, Pedchenko V, Hudson BG. Mammalian collagen IV. Microscopy Research and Technique. 2008;71(5):357–70.

[9] Mouw JK, Ou G, Weaver VM. Extracellular matrix assembly: a multiscale deconstruction. Nature Reviews Molecular Cell Biology. 2014;15(12):771–85.

[10] Alberts B, et al. Molecular biology of the cell. 4th ed. Garland Science, New York; 2002.

[11] Yurchenco PD, Patton BL. Developmental and pathogenic mechanisms of basement membrane assembly. Current Pharmaceutical Design. 2009;15(12):1277–94.

[12] Kalluri R. Basement membranes: structure, assembly and role in tumour angiogenesis. Nature Reviews Cancer. 2003;3(6):422–33.

[13] Tilling T, Korte D, Hoheisel D, Galla HJ. Basement membrane proteins influence brain capillary endothelial barrier function in vitro. Journal of Neurochemistry. 1998;71(3): 1151–7.

[14] Iozzo RV. Matrix proteoglycans: from molecular design to cellular function. Annual Review of Biochemistry. 1998;67:609–52.

[15] Kresse H, Schonherr E. Proteoglycans of the extracellular matrix and growth control. Journal of Cell Physiology. 2001;189(3):266–74.

[16] Yanagishita M. Function of proteoglycans in the extracellular-matrix. Acta Pathology Japan. 1993;43(6):283–93.

[17] Streuli C. Extracellular matrix remodelling and cellular differentiation. Current Opinion in Cell Biology. 1999;11(5):634–40.

[18] Werb Z. ECM and cell surface proteolysis: regulating cellular ecology. Cell. 1997;91(4): 439–42.

[19] Gu ZZ, Cui J, Brown S, Fridman R, Mobashery S, Strongin AY, et al. A highly specific inhibitor of matrix metalloproteinase-9 rescues laminin from proteolysis and neurons from apoptosis in transient focal cerebral ischemia. Journal of Neuroscience. 2005;25(27):6401–8.

[20] Wang CX, Shuaib A. Critical role of microvasculature basal lamina in ischemic brain injury. Progress in Neurobiology. 2007;83(3):140–8.

[21] Kitajewski J. Endothelial laminins underlie the tip cell microenvironment. Embo Reports. 2011;12(11):1087–8.

[22] Timpl R, Brown JC. The laminins. Matrix Biology. 1994;14(4):275–81.

[23] Poschl E, Schlotzer-Schrehardt U, Brachvogel B, Saito K, Ninomiya Y, Mayer U. Collagen IV is essential for basement membrane stability but dispensable for initiation of its assembly during early development. Development. 2004;131(7):1619–28.

[24] Holster T, Pakkanen O, Soininen R, Sormunen R, Nokelainen M, Kivirikko KI, et al. Loss of assembly of the main basement membrane collagen, type IV, but not fibril-forming collagens and embryonic death in collagen prolyl 4-hydroxylase I null mice. The Journal of Biological Chemistry. 2007;282(4):2512–9.

[25] Kang SH, Kramer JM. Nidogen is nonessential and not required for normal type IV collagen localization in *Caenorhabditis elegans*. Molecular Biology of the Cell. 2000;11(11):3911–23.

[26] Murshed M, Smyth N, Miosge N, Karolat J, Krieg T, Paulsson M, et al. The absence of nidogen 1 does not affect murine basement membrane formation. Molecular and Cellular Biology. 2000;20(18):7007–12.

[27] Schymeinsky J, Nedbal S, Miosge N, Poschl E, Rao C, Beier DR, et al. Gene structure and functional analysis of the mouse nidogen-2 gene: nidogen-2 is not essential for basement membrane formation in mice. Molecular and Cellular Biology. 2002;22(19):6820–30.

[28] Willem M, Miosge N, Halfter W, Smyth N, Jannetti I, Burghart E, et al. Specific ablation of the nidogen-binding site in the laminin gamma1 chain interferes with kidney and lung development. Development. 2002;129(11):2711–22.

[29] To M, Goz A, Camenzind L, Oertle P, Candiello J, Sullivan M, et al. Diabetes-induced morphological, biomechanical, and compositional changes in ocular basement membranes. Experimental Eye Research. 2013;116:298–307.

[30] Cecchelli R, Berezowski V, Lundquist S, Culot M, Renftel M, Dehouck MP, et al. Modelling of the blood–brain barrier in drug discovery and development. Nature Reviews Drug Discovery. 2007;6(8):650–61.

[31] Lieleg O, Ribbeck K. Biological hydrogels as selective diffusion barriers. Trends in Cell Biology. 2011;21(9):543–51.

[32] Proksch E, Brandner JM, Jensen JM. The skin: an indispensable barrier. Experimental Dermatology. 2008;17(12):1063–72.

[33] Sebinger DDR, Ofenbauer A, Gruber P, Malik S, Werner C. ECM modulated early kidney development in embryonic organ culture. Biomaterials. 2013;34(28):6670–82.

[34] Miner JH. Renal basement membrane components. Kidney International. 1999;56(6):2016–24.

[35] Ballabh P, Braun A, Nedergaard M. The blood–brain barrier: an overview—structure, regulation, and clinical implications. Neurobiology of Disease. 2004;16(1):1–13.

[36] Gabe SM. Gut barrier function and bacterial translocation in humans. Clinical Nutrition. 2001;20:107–12.

[37] Tsang KY, Cheung MC, Chan D, Cheah KS. The developmental roles of the extracellular matrix: beyond structure to regulation. Cell Tissue Research. 2010;339(1):93–110.

[38] Benton G, Kleinman HK, George J, Arnaoutova I. Multiple uses of basement membrane-like matrix BME/Matrigel) in vitro and in vivo with cancer cells. International Journal of Cancer. 2011;128(8):1751–7.

[39] Godin AG, Lounis B, Cognet L. Super-resolution microscopy approaches for live cell imaging. Biophysical Journal. 2014;107(8):1777–84.

[40] Koh HS, Yong T, Chan CK, Ramakrishna S. Enhancement of neurite outgrowth using nano-structured scaffolds coupled with laminin. Biomaterials. 2008;29(26):3574–82.

[41] Hidalgo-Bastida LA, Barry JJ, Everitt NM, Rose FR, Buttery LD, Hall IP, et al. Cell adhesion and mechanical properties of a flexible scaffold for cardiac tissue engineering. Acta Biomaterialia. 2007;3(4):457–62.

[42] Kleinman HK, Mcgarvey ML, Hassell JR, Star VL, Cannon FB, Laurie GW, et al. Basement-membrane complexes with biological-activity. Biochemistry. 1986;25(2): 312–8.

[43] Kleinman HK, Mcgarvey ML, Liotta LA, Robey PG, Tryggvason K, Martin GR. isolation and characterization of type-iv procollagen, laminin, and heparan-sulfate proteoglycan from the EHS sarcoma. Biochemistry. 1982;21(24):6188–93.

[44] Vukicevic S, Luyten FP, Kleinman HK, Reddi AH. Differentiation of canalicular cell processes in bone-cells by basement-membrane matrix components—regulation by discrete domains of laminin. Cell. 1990;63(2):437–45.

[45] Li ML, Aggeler J, Farson DA, Hatier C, Hassell J, Bissell MJ. Influence of a reconstituted basement-membrane and its components on casein gene-expression and secretion in mouse mammary epithelial-cells. Proceedings of the National Academy of Sciences of the United States of America. 1987;84(1):136–40.

[46] Kibbey MC, Royce LS, Dym M, Baum BJ, Kleinman HK. Glandular-like morphogenesis of the human submandibular tumor cell line A253 on basement membrane components. Experimental Cell Research. 1992;198(2):343–51.

[47] Hadley MA, Byers SW, Suarezquian CA, Kleinman HK, Dym M. Extracellular-matrix regulates Sertoli-cell differentiation, testicular cord formation, and germ-cell development in vitro. Journal of Cell Biology. 1985;101(4):1511–22.

[48] Zaman MH, Trapani LM, Siemeski A, MacKellar D, Gong H, Kamm RD, et al. Migration of tumor cells in 3D matrices is governed by matrix stiffness along with cell-matrix

adhesion and proteolysis (vol. 103, p. 10889, 2006). Proceedings of the National Academy of Sciences of the United States of America. 2006;103(37):13897.

[49] Valster A, Tran NL, Nakada M, Berens ME, Chan AY, Symons M. Cell migration and invasion assays. Methods. 2005;37(2):208–15.

[50] Arends F, Nowald C, Pflieger K, Boettcher K, Zahler S, Lieleg O (2015) The Biophysical Properties of Basal Lamina Gels Depend on the Biochemical Composition of the Gel. PloS ONE 10(2): e0118090. doi:10.1371/journal.pone.0118090

[51] Lieleg O, Claessens MMAE, Bausch AR. Structure and dynamics of cross-linked actin networks. Soft Matter. 2010;6(2):218–25.

[52] Engler AJ, Sen S, Sweeney HL, Discher DE. Matrix elasticity directs stem cell lineage specification. Cell. 2006;126(4):677–89.

[53] Massensini AR, Ghuman H, Saldin LT, Medberry CJ, Keane TJ, Nicholls FJ, et al. Concentration-dependent rheological properties of ECM hydrogel for intracerebral delivery to a stroke cavity. Acta Biomaterialia. 2015;27:116–30.

[54] Chen DTN, Wen Q, Janmey PA, Crocker JC, Yodh AG. Rheology of soft materials. Annu. Rev. Condens. Matter Phys. 2010;1:301–22.

[55] Takeyasu K. Atomic force microscopy in nanobiology, Pan Stanford Publishing Pte. Ltd., Singapore, 2014

[56] Luan Y, Lieleg O, Wagner B, Bausch AR. Micro- and macrorheological properties of isotropically cross-linked actin networks. Biophysics Journal. 2008;94(2):688–93.

[57] Lu L, Oswald SJ, Ngu H, Yin FCP. Mechanical properties of actin stress fibers in living cells. Biophysical Journal. 2008;95(12):6060–71.

[58] Kirmizis D, Logothetidis S. Atomic force microscopy probing in the measurement of cell mechanics. International Journal of Nanomedicine. 2010;5:137–45.

[59] Nia HT, Bozchalooi IS, Li Y, Han L, Hung HH, Frank E, et al. High-bandwidth AFM-based rheology reveals that cartilage is most sensitive to high loading rates at early stages of impairment. Biophysical Journal. 2013;104(7):1529–37.

[60] Candiello J, Balasubramani M, Schreiber EM, Cole GJ, Mayer U, Halfter W, et al. Biomechanical properties of native basement membranes. The FEBS Journal. 2007;274(11):2897–908.

[61] Last JA, Liliensiek SJ, Nealey PF, Murphy CJ. Determining the mechanical properties of human corneal basement membranes with atomic force microscopy. Journal of Structural Biology. 2009;167(1):19–24.

[62] Valentine MT, Perlman ZE, Gardel ML, Shin JH, Matsudaira P, Mitchison TJ, et al. Colloid surface chemistry critically affects multiple particle tracking measurements of biomaterials. Biophysical Journal. 2004;86(6):4004–14.

[63] Lieleg O, Baumgärtel RM, Bausch AR. Selective filtering of particles by the extracellular matrix: an electrostatic bandpass. Biophysical Journal. 2009;97(6):1569–77.

[64] Hunter RJ. Zeta potential in colloid science: principles and applications. Academic Press, London; 1989.

[65] Arends F, Baumgartel R, Lieleg O. Ion-specific effects modulate the diffusive mobility of colloids in an extracellular matrix gel. Langmuir: the ACS Journal of Surfaces and Colloids. 2013;29(51):15965–73.

[66] Arends F, Sellner S, Seifert P, Gerland U, Rehberg M, Lieleg O. A microfluidics approach to study the accumulation of molecules at basal lamina interfaces. *Lab Chip*, 2015,, 3326–3334., 15

[67] Kaemmerer E, Melchels FP, Holzapfel BM, Meckel T, Hutmacher DW, Loessner D. Gelatine methacrylamide-based hydrogels: an alternative three-dimensional cancer cell culture system. Acta Biomaterialia. 2014;10(6):2551–62.

[68] Seto SP, Casas ME, Temenoff JS. Differentiation of mesenchymal stem cells in heparin-containing hydrogels via coculture with osteoblasts. Cell Tissue Research. 2012;347(3): 589–601.

[69] Chauhan VP, Stylianopoulos T, Boucher Y, Jain RK. Delivery of molecular and nanoscale medicine to tumors: transport barriers and strategies. Annual Review of Chemical and Biomolecular. 2011;2:281–98.

[70] Holback H, Yeo Y. Intratumoral drug delivery with nanoparticulate carriers. Pharmaceutical Research. 2011;28(8):1819–30.

[71] Ernsting MJ, Murakami M, Roy A, Li SD. Factors controlling the pharmacokinetics, biodistribution and intratumoral penetration of nanoparticles. Journal Controlled Release. 2013;172(3):782–94.

[72] Bertrand N, Wu J, Xu X, Kamaly N, Farokhzad OC. Cancer nanotechnology: the impact of passive and active targeting in the era of modern cancer biology. Advanced Drug Delivery Reviews. 2014;66:2–25.